Pergamon

Cement and Concrete Research, Vol. 28, No. 11, pp. 1669–1681, 1998

0008-8846/98 $19.00 + .00

PII S0008-8846(98)00138-0

DISAPPEARANCE OF OXYGEN IN CONCRETE UNDER IRRADIATION: THE ROLE OF PEROXIDES IN RADIOLYSIS

P. Bouniol[1] and A. Aspart
Commissariat à l'Energie Atomique, DCC/DESD/SESD, CEA-Saclay 91191 Gif sur Yvette Cedex, France

(Received August 8, 1998; in final form August 19, 1998)

ABSTRACT

Under irradiation, the interstitial liquid in concretes is affected by radiolysis. Normally produced with H_2 in alkaline medium, O_2 is not observed. It is shown that the disappearance of O_2 results not only from the fast reaction with the e^-_{aq} radical, which causes a negative redox potential, but also from peroxide trapping in $CaO_2{\cdot}8H_2O$, a highly insoluble phase whose solubility product is estimated at 2.8×10^{-11}. The disequilibrium that occurs in the redox sequence dioxygen (0) $\leftrightarrow$ superoxide ($-½$) $\leftrightarrow$ peroxide (-1) is responsible for depleting most of the oxygenated species in the solution. $CaO_2{\cdot}8H_2O$ is formed at the expense of calcium in solution, of portlandite, and of ettringite, but, being unstable, it disappears in the cement paste when H_2O_2 is no longer present in the medium. Consideration of the reaction between $Ca(OH)_2$ and H_2O_2 in the CHEMSIMUL kinetic code, which also highlights O_2 consumption, seems to describe the long-term radiolysis of concrete accurately.

Introduction

Among the many nuclear applications of concrete, radioactive waste conditioning occupies a special position, because of original service conditions and the safety objectives associated with the duration of the structures. For long-lived wastes (class B, low and medium level and alpha emitters $> 3.7 \times 10^6$ Bq kg^{-1}), the cement-based materials are required to undergo either mixed $\alpha\beta\gamma$ irradiation as an immobilization matrix, or external γ irradiation as a container material.

In these two configurations, the interstitial liquid and the molecular water associated with the hydrates are affected by radiolysis, a radiochemical mechanism that causes the evolution of gas in situ. The two risks resulting from radiolysis, internal overpressure with cracking of the packages and the accumulation of explosive gas (H_2) in a storage area, have sparked most of the investigations on the elementary mechanisms occurring in concrete under irradiation.

Among the areas that restrict our understanding of the mechanisms, if only for a comprehensive description of radiolysis, the singular behavior of oxygen appears crucial. In fact,

[1]To whom correspondence should be addressed.

TABLE 1
βγ primary yields at pH 13 with the convention $e^-_{aq} \equiv H_2O^-$.

Radiolytic species	H_2	e^-_{aq}	H	OH^-	H_2O	H^+	OH	H_2O_2
G species	0.425	2.8	0.55	0.5	−7.50	3.30	3.0	0.6

The values (molecules/100 eV) must be multiplied by 1.036×10^{-7} to obtain G in mol J^{-1} (4).

most investigations agree that dioxygen disappears rapidly during the irradiation of cement-based materials (1,2). Although the cause of this process is still unexplained, it is an integral part of the radiolytic processes. Hence, it appears difficult to describe the quantities of H_2 produced or the pressures reached by a cement matrix if the O_2 consumption mechanism is not clearly understood.

General

Radiolysis is the physicochemical consequence of ionizations on the water molecule after the passage of radiation. With respect to this mechanism, the interstitial aqueous phase is the weak point of the concrete, and the macroscopic disorders induced appear to predominate over microscopic events such as intracrystalline defects, amorphization, or demixing, caused by atomic displacements.

After 10^{-7} seconds, ionization and, to a lesser degree, electronic excitations result in the appearance of primary products of a molecular or ionic nature (H_2, H_2O_2, H^+, OH^-: stable) or free-radical nature (e^-_{aq}, H, OH: highly unstable). Their respective yields (denoted as G), i.e., the quantities produced related to the energy deposited in the mass of water, are known (3,4) for alkaline media (Table 1).

The primary products then react with the solutes present in the interstitial liquid, particularly OH^-, producing new species with a complex chemistry: O^-, $O_2{}^-$, HO_2, $HO_2{}^-$, etc. In this arrangement, O_2, unlike H_2, is not a primary product after radiolysis of water, but nevertheless may be formed by side reactions:

$$O^- + O_2{}^- + H_2O \rightarrow 2OH^- + O_2 \quad k = 6 \times 10^8 \text{ kg mol}^{-1} \text{ s}^{-1} \quad (5)$$
$$OH + O_2{}^- \rightarrow OH^- + O_2 \quad k = 1 \times 10^{10} \text{ kg mol}^{-1} \text{ s}^{-1} \quad (5)$$
$$HO_2 + O_2{}^- \rightarrow HO_2{}^- + O_2 \quad k = 9.7 \times 10^7 \text{ kg mol}^{-1} \text{ s}^{-1} \quad (5)$$
$$H^+ + O_3{}^- \rightarrow OH + O_2 \quad k = 9 \times 10^{10} \text{ kg mol}^{-1} \text{ s}^{-1} \quad (5)$$

In an alkaline solution such as the aqueous phase of concrete, O_2 should consequently be observed, but this occurs only exceptionally.

The direct disappearance of O_2 results from the attack of the e^-_{aq} radicals and, to a lesser extent, of the O^- radicals specific to the alkaline medium:

$$e^-_{aq} + O_2 \rightarrow H_2O + O_2{}^- \quad k = 1.9 \times 10^{10} \text{ kg mol}^{-1} \text{ s}^{-1} \quad (5)$$
$$O^- + O_2 \rightarrow O_3{}^- \quad k = 3.6 \times 10^9 \text{ kg mol}^{-1} \text{ s}^{-1} \quad (5)$$

If the cement-based materials already contain dioxygen when irradiation begins, the latter mechanism explains the rapid disappearance of O_2 that is routinely observed. The mecha-

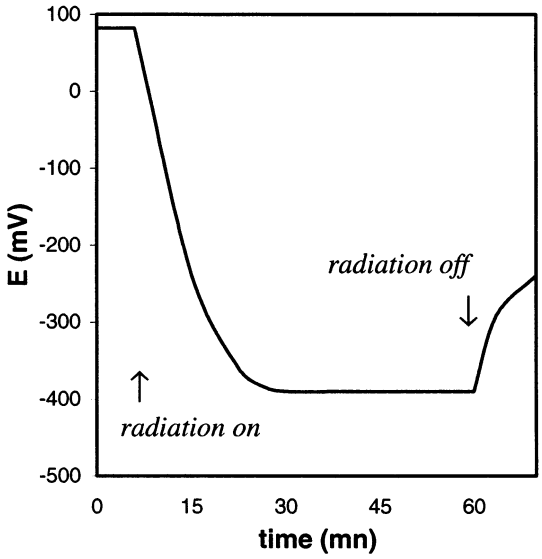

FIG. 1.
Electrode potential of Portland cement paste under γ irradiation, after reference (6).

nisms governing the disappearance of the dioxygen also have been examined in this configuration (6): from the crushed material of pure Portland cement paste in distilled water conditioned in a sealed ampule, the redox potential was monitored sheltered from air before, during, and after irradiation, using a Pt-Ag/AgCl electrode. Irradiation (γ ^{60}Co) was applied with a dose rate of 0.78 Gy s^{-1}. Starting with a positive potential between $+0.05$ and $+0.1$ V (H_2 reference), normally associated with 9 ppm of dioxygen dissolved in initial equilibrium with the atmosphere, the medium displays a rapid drop in potential under irradiation, reaching values of -0.4 or even -0.7 V (Fig. 1). The disappearance of O_2 is observed simultaneously (gas chromatography).

Whereas the interpretation of (6) applies equally well to surface absorption of O_2, the oxidation of a reducing species in "cement water," or the stabilization of a radiolytic species of oxygen by C-S-H gel [peroxy-gel (7)], it now appears that the negative change in the redox potential is controlled by the O_2^-/O_2 pair ($E° = -0.33$ V, independent of the pH in alkaline medium, Fig. 2) and that the degree of oxidation thus gained by the oxygen ($-½$) is not the ultimate step in the mechanism.

In fact, when the irradiation conditions become anaerobic, the formation of water should be observed again, because the relatively weak reactivity of the O_2^- ion (superoxide) in aprotic media leads to an accumulation such that it becomes the majority free-radical species. In these conditions, the formation of O_2 by O_2^- is higher than the consumption of O_2 by e^-_{aq} (in addition, this latter gives back O_2^-).

In anaerobic conditions, a new mechanism must be enlisted to explain not the disappearance, but the nonappearance of the dioxygen. In this connection, even if the O_2^- ion occupies a predominant role, it only represents an intermediate species in the chemistry of oxygenated

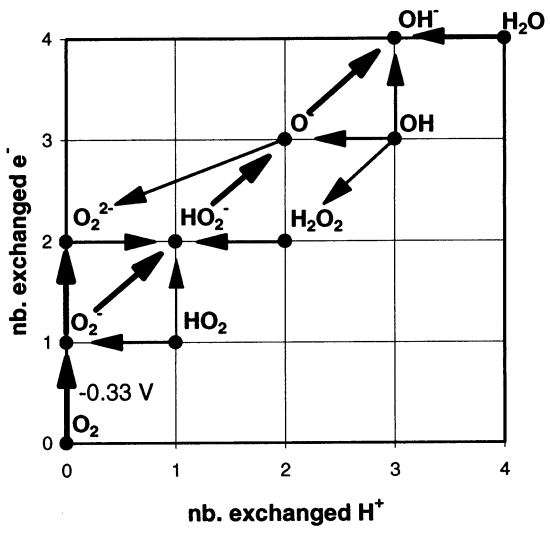

FIG. 2.
Redox and acid–base equilibria of oxygenated species from radiolysis of water in alkaline medium.

species, because the true precursors are H_2O_2 and its basic homologue HO_2^-, i.e., peroxides (oxidation degree -1):

$$O^- + HO_2^- \rightarrow OH^- + O_2^- \quad k = 4 \times 10^8 \text{ kg mol}^{-1} \text{ s}^{-1} \quad (5)$$
$$OH + HO_2^- \rightarrow OH^- + HO_2 \quad k = 8.3 \times 10^9 \text{ kg mol}^{-1} \text{ s}^{-1} \quad (5)$$

The following reversible equations supplement the foregoing equations:

$$HO_2 + OH^- \leftrightarrow H_2O + O_2^- \quad pK_a = 4.8 \quad (8)$$
$$H_2O_2 + OH^- \leftrightarrow H_2O + HO_2^- \quad pK_a = 11.65 \quad (9)$$
$$OH + OH^- \leftrightarrow H_2O + O^- \quad pK_a = 11.9 \quad (10)$$

As the primary product, H_2O_2 is systematically formed during radiolysis and can be considered to be the main oxygenated species in the irradiated aqueous solutions. The mobilization of the peroxides in nonradiolytic reactions involving a major solute of the cement accordingly appears to be the possible cause of the absence of O_2 in irradiated concretes. We recently suggested that the major reaction of the cement calcium (in ionic or solid form) with H_2O_2 was responsible for the precipitation of calcium peroxide thus fixing oxygen (11).

Experimental

The identification of calcium peroxide in the cement paste after radiolysis is a difficult matter due to the metastable character of this compound and the small amount formed. The species

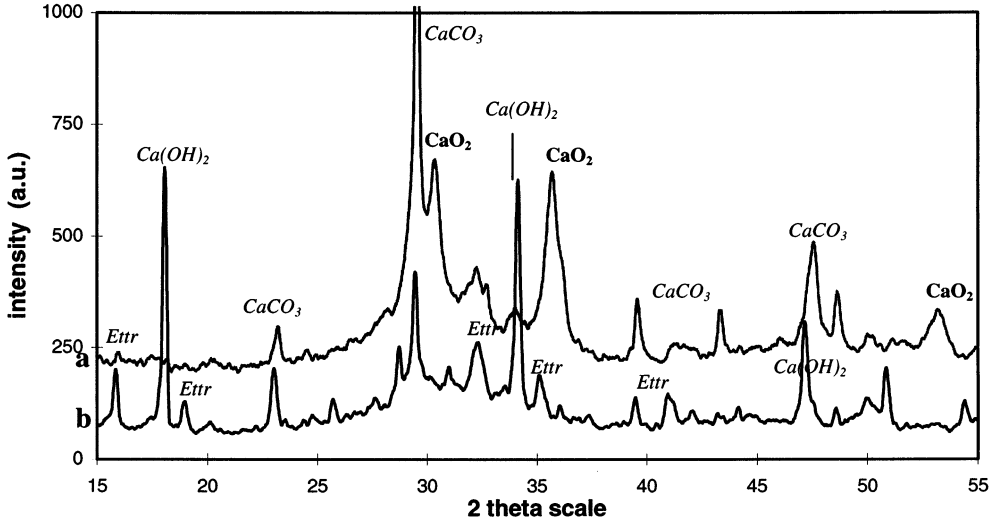

FIG. 3.
X-ray diffraction spectra of Portland cement pastes. (*a*) Attack by H_2O_2; (*b*) reference. Ettr, ettringite.

theoretically obtained is the peroxide octahydrate (12,13), which can be produced easily in aqueous solution in the presence of calcium and H_2O_2:

$$Ca(OH)_{2\,aq} + H_2O_{2\,aq} + 6H_2O \rightarrow CaO_2{\cdot}8H_2O \downarrow$$

It is a pearly white solid crystallizing in the tetragonal system, very slightly soluble, but capable of easily losing its water of crystallization in air and then decomposing with simultaneous carbonation (12):

$$CaO_2{\cdot}8H_2O \rightarrow CaO_2 + 8H_2O$$

$$CaO_2 + H_2O \rightarrow Ca(OH)_2 + \tfrac{1}{2}O_2$$

$$Ca(OH)_2 + CO_2 \rightarrow CaCO_3 + H_2O$$

To demonstrate the formation of Ca peroxide in the alkaline context of "concrete," the direct attack of a Portland cement paste aged 18 months (water/cement = 0.4) by an aqueous solution containing 30 wt% H_2O_2 ($[H_2O_2] = 12.6$ mol kg^{-1}) was carried out. The completely hydrated paste, protected from carbonation, was ground and introduced into excess H_2O_2 solution. Effervescence occurred simultaneously with the appearance of a slight brown color on the solid phase. After 12 h, the reaction product was sampled, dried under vacuum, and examined by x-ray diffraction: carbonation is unavoidable at this stage.

Comparison of the spectrum obtained with that of a reference paste reveals (Fig. 3):

- the appearance of three characteristic peaks of anhydrous tetragonal CaO_2 (datasheet JCPDS 3-0865),

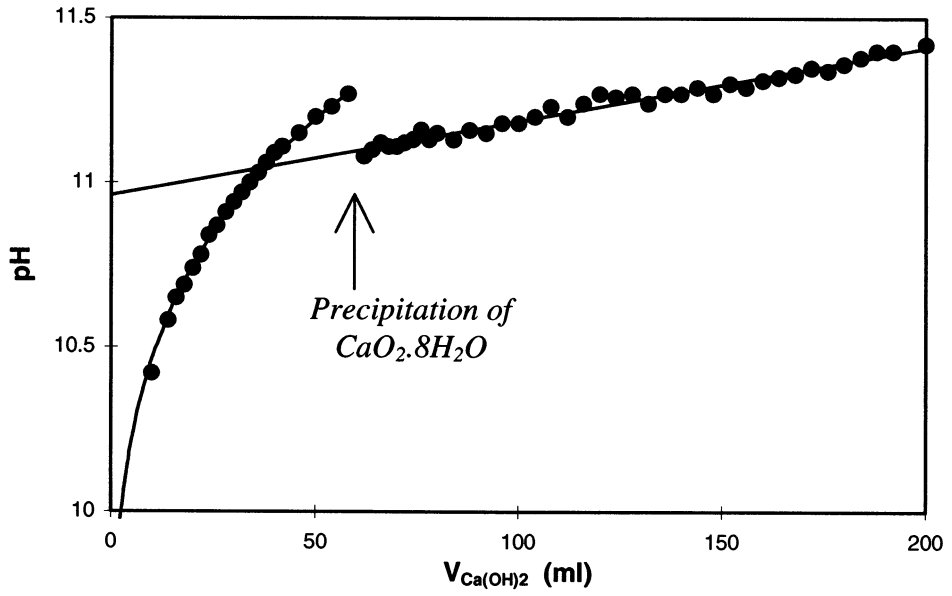

FIG. 4.
Curve of neutralization of H_2O_2 solution by saturated $Ca(OH)_2$ solution.

- the disappearance of portlandite and ettringite, and
- a tendency to carbonation.

The mobilization of calcium to form peroxide thus occurs at the expense of portlandite and ettringite, which normally makes sampling more difficult from C-S-H. The same operation, performed with very pure portlandite, serves to obtain a better crystallized CaO_2, which has a slightly longer (few weeks) lifetime at 20°C if protected from air.

If the massive input of H_2O_2 causes a reaction with calcium of the solid phase, the progressive input as occurs during radiolysis necessarily concerns calcium in the liquid phase. The solubility of $CaO_2{\cdot}8H_2O$ must therefore be known. To determine this solubility, 240 ± 1 mL of an aqueous solution of 0.02 M H_2O_2 was titrated by successive additions of a saturated solution of $Ca(OH)_2$ (Radiometer® buffer solution pH 12.45 at 0.021 mol kg^{-1}). The reaction was monitored by a pH electrode in a double-jacketed Pyrex reactor, thermostatically controlled at 25.0 ± 0.2°C under a decarbonated nitrogen flow.

The change in the pH displays a first and typical portion of acid–base neutralization, succeeded by a straight portion, the difference between the two corresponding to the time when $CaO_2{\cdot}8H_2O$ precipitates in the solution (Fig. 4). Adjustment of the experimental points gives, respectively:

- Before precipitation: $pH = 8.53556 + 1.21515\ (V_{Ca(OH)_2})^{1/5}$
- After precipitation: $pH = 10.9614 + 2.24649 \times 10^{-3}\ V_{Ca(OH)_2}$

TABLE 2
Equilibria and electroneutrality equation to be considered in calculating the solubility product of $CaO_2 \cdot 8H_2O$.

$Ca2^+ + OH^- \Leftrightarrow CaOH^+$	$K_1 = 10^{1.299}$
$CaOH^+ + OH^- \Leftrightarrow Ca(OH)_2°$	$K_2 = 10^{-1.07}$
$H_2O_2 \Leftrightarrow HO_2^- + H^+$	$K_3 = 10^{-11.65}$ [9]
$HO_2^- \Leftrightarrow O_2^{2-} + H^+$	$K_4 = 10^{-16.5}$ [15]
$H_2O \Leftrightarrow OH^- + H^+$	$K_w = 10^{-13.995}$
$CaO_2 \Leftrightarrow Ca^{2+} + O_2^{2-}$	$K_{per} = (Ca^{2+}) \cdot (O_2^{2-})$
$[OH^-] + [HO_2^-] + 2[O_2^{2-}] = [H^+] + [CaOH^+] + 2[Ca^{2+}]$	

The equalization of the foregoing functions helps to determine the pH and the quantity of calcium, which define the theoretical start of precipitation, or pH = 11.046 and $V_{Ca(OH)_2}$ = 37.63 mL, implying a total analytical concentration $\Sigma[Ca] = 2.91 \times 10^{-3}$ mol kg^{-1}. These results, combined with the equations governing the equilibria between calcium or peroxide species on the one hand, with the ionic product of water and with the electroneutrality equation on the other (Table 2), help to calculate the solubility product of CaO_2"$8H_2O$ and the total peroxide concentration by iteration of the ionic strength:

$$K_{per} = [Ca^{2+}] \cdot [O_2^{2-}] \cdot \gamma_2^2 = 2.8 \times 10^{-11}$$

$$\Sigma[\text{peroxide}] = [H_2O_2] + [HO_2^-] + [O_2^{2-}] = 2.1 \times 10^{-2} \text{ mol kg}^{-1}$$

Considering an ionic strength lower than 10^{-2} mol kg^{-1}, the activity coefficients γ_1 and γ_2 are calculated with the Davies equation.

Taking, for example, the characteristics of an interstitial liquid of ordinary Portland cement paste (Table 3), we find that the solubility product is reached at a fairly low peroxide ion concentration: $[O_2^{2-}] = 4.58 \times 10^{-7}$ mol kg^{-1}. In these conditions, even considering supersaturation of the liquid corresponding to slightly more than three times the solubility product (as in the present experiment), $CaO_2 \cdot 8H_2O$ is caused to precipitate fairly rapidly in the cement paste under irradiation. Considering the primary yield $G_{H_2O_2}$ (6.216×10^{-8} mol J^{-1}), the solubility product K_{per}, the speciation of the peroxides in alkaline medium, and their preservation from the free radicals of radiolysis, a threshold dose corresponding to the precipitation of $CaO_2 \cdot 8H_2O$ can be estimated from the following equations:

TABLE 3
Characteristics of the interstitial liquid of an ordinary Portland cement paste at 25°C (11)

Ionic strength: $I = 0.2439$ mol kg^{-1}	Activity coefficients: $\gamma_1 = 0.7395$, $\gamma_2 = 0.2990$
pH = 13.244	$\rho_{liq} = 1007.8$ kg m^{-3}
$\Sigma[Ca] = 2.04 \times 10^{-3}$ mol kg^{-1}	$\Sigma[A_i] = [H_2O] + [\text{solutes}] = 55.992$ mol kg^{-1}
$[Ca^{2+}] = 6.85 \times 10^{-4}$ mol kg^{-1}	$\Sigma \mathcal{M}_i[A_i] = 1.012$ ($\text{mass}_{solution}/\text{mass}_{solvent}$)

$$[O_2^{2-}] = \frac{K_3K_4[H_2O_2]}{\gamma_2\gamma_1^2[H^+]^2} \qquad \text{(from Table 2)}$$

$$K_{per} = [Ca^{2+}][O_2^{2-}]\cdot\gamma_2^2 \qquad \text{(by definition)}$$

$$\gamma_1[H^+] = 10^{-pH} \qquad \text{(by definition)}$$

$$[H_2O_2] = G_{H_2O_2} \times \text{dose} \qquad \text{(by definition)}$$

This gives:

$$\text{Dose}_{\text{threshold}} = \frac{K_{per}\cdot 10^{-2pH}}{K_3K_4\gamma_2\cdot[Ca^{2+}]\cdot G_{H_2O_2}} \approx 100 \text{ grays}$$

Insofar as the doses integrated by the cement matrices in geological disposal, or during irradiaton experiments, will rapidly exceed this value, the precipitation of Ca peroxide can be considered systematically in modeling radiolysis.

Model

The evaluation of the gas partial pressures reached in the pores of the concrete under radiation is one of the main objectives of the model. This is performed using the CHEMSIMUL program (14), a kinetic code especially designed for the numerical processing of the system of differential equations resulting from the radiolytic reactions of water (more than 60 with acid–base reactions and phase changes of the $O_{2\ aq} \Leftrightarrow O_{2\ g}$ type). In the present case, the list of reactions conventionally admitted (3) is supplemented by a simplified "calcium" module consisting of three "reactions":

$\text{Portlandite} \rightarrow Ca(OH)_{2\ aq}$	$k = 2.04 \times 10^5\ s^{-1}$
$Ca(OH)_{2\ aq} \rightarrow \text{portlandite}$	$k = 1 \times 10^{10}\ s^{-1}$
$Ca(OH)_{2\ aq} + H_2O_2 \rightarrow CaO_2 + 2H_2O$	$k = 5 \times 10^7\ \text{kg mol}^{-1}$

The first two, combined with the initial portlandite and $Ca(OH)_{2\ aq}$ concentrations equal to 100 (arbitrary) and 2.04×10^{-3} mol kg^{-1}, respectively, assume instantaneous and permanent equilibrium between a virtually inexhaustible source of solid calcium and the interstitial liquid in which the total concentration Ca remains constant. The treatment of $[Ca(OH)_{2\ aq}]$ as $\Sigma[Ca]$ is an expedient here, to avoid treating the speciation of calcium and the associated reaction kinetics, which are mostly unknown. The third reaction reflects the overall attack of calcium by H_2O_2 and the formation of peroxide with a relatively low rate constant.

Reference (15) also helps to clarify the kinetics of O_2^{2-} disappearance, a species normally considered as nonexistent in water, because it is a stronger base than OH^-. With a pK_a slightly higher than 16 and a rate constant of O_2^{2-} attack by water higher than 2×10^5 kg mol^{-1} s^{-1}, the O_2^{2-} concentrations at pH $\geq$ 13 actually becomes significant and the following acid–base equilibrium must by introduced into CHEMSIMUL:

$$O_2^{2-} + H_2O \underset{k2}{\overset{k1}{\rightleftharpoons}} HO_2^- + OH^-$$

At equilibrium:

$$k_1 \cdot [O_2^{2-}][H_2O] = k_2 \cdot [HO_2^-][OH^-] \Rightarrow k_2^0 = k_1 \cdot \frac{K_4}{K_w} \cdot [H_2O]$$

(zero ionic strength)

Assuming $k_1 = 5 \times 10^5$ kg mol^{-1} s^{-1} and by correcting the constant of the ionic strength by the Bronsted–Bjerrum equation, we obtain:

$$k_2 = \frac{k_2^0}{\gamma_1^2} = 1.59 \times 10^5 \text{ kg mol}^{-1} \text{ s}^{-1}$$

(reaction between charged species of the same sign)

It is especially important to consider the reactions leading to the by-production of the peroxide ion in alkaline medium:

$$O^- + O^- \rightarrow O_2^{2-} \qquad k = 1.0 \times 10^8 \text{ kg mol}^{-1} \text{ s}^{-1} \quad [16]$$
$$e^-_{aq} + O_2^- \rightarrow H_2O + O_2^{2-} \qquad k = 1.3 \times 10^{10} \text{ kg mol}^{-1} \quad [5]$$

Although CHEMSIMUL covers the basis of homogeneous reactions in solution, "heterogeneous" reactions can be managed, reflecting the degassing and resolubilization mechanisms, which are indispensable for describing the changes in pressures over time. The kinetic constants of these first-order reactions have an identical expression for each gas j:

$$\text{Degassing } (J_{aq} \rightarrow J_g): \qquad k_{1j} = \frac{\mathcal{A}}{V_{liq}} \cdot k_{wj}$$

$$\text{Solubilization } (J_g \rightarrow J_{aq}): \quad k_{2j} = k_{1j} \cdot \frac{V_{liq}}{V_{gas}} \cdot \frac{RT}{K_j} \cdot \frac{\rho_{liq} \sum_i [A_i]}{\sum_i \mathcal{M}_i [A_i]}$$

In these equations, j denotes H_2, O_2, N_2, or H_2O vapor, where:

$\mathcal{A}$ = liquid–gas interfacial area (m^2)
k_{wj} = interface transfer coefficient (m s^{-1})
K_j = Henry coefficient (Pa)
V_{gas}, V_{liq} = volumes of gas and liquid making up the pores (m^3)
RT = ideal gas constant × temperature (J mol^{-1})

By treating the equilibria $J_{aq} \Leftrightarrow J_g$ as any homogeneous equilibrium, CHEMSIMUL calculates the concentrations $[J_{aq}]$ and $[J_g]$, helping to obtain the partial pressure:

$$P(J) = [J_g] \cdot \frac{RT\rho_{liq}}{\sum_i \mathcal{M}_i [A_i]} \cdot \frac{V_{liq}}{V_{gas}}$$

Considering a pure Portland cement paste in a confined cylindrical specimen (D = 11 cm and h = 22 cm), with a porosity occupied in equal shares by the liquid and gas phases

TABLE 4
Geometric characteristics, transfer coefficients after (17), and Henry coefficients selected for the simulation of the radiolysis of a Portland cement paste w/c $\approx$ 0.36 at 25°C.

Total volume: $V_{tot} = 2.2 \times 10^{-3}$ m^3 Porosity: $n = 0.3$
Interfacial area: $\mathcal{A} = 1.82 \times 10^{4}$ m^2

$$\frac{V_{gas}}{V_{liq}} = 1 \Rightarrow V_{gas} = V_{liq} = \frac{n \cdot V_{tot}}{2} = 3.3 \times 10^{-4} \text{ m}^3$$

$k_{wH_2} = 1.389 \times 10^{-6}$ m s^{-1}	$K_{H_2} = 7.181 \times 10^{9}$ Pa	$R = 8.3144$ J mol^{-1} K^{-1}
$k_{wO_2} = 1.153 \times 10^{-6}$ m s^{-1}	$K_{O_2} = 4.419 \times 10^{9}$ Pa	$T = 298.15$ K
$k_{wN_2} = 9.747 \times 10^{-7}$ m s^{-1}	$K_{H_2} = 8.565 \times 10^{9}$ Pa	
$k_{wH_2O} = 1.278 \times 10^{-6}$ m s^{-1}	$K_{H_2O} = 3.169 \times 10^{3}$ Pa	

(physicochemical and geometric characteristics given in Tables 3 and 4), the partial pressure of each gas is calculated for a γ dose rate of 0.01 Gy s^{-1} if the Ca/H_2O_2 reaction is taken into account and if not. Assuming an initial total pressure equal to the atmospheric pressure, the change in the system over 1 year displays the shape of Figures 5A and 5B, respectively. In the former case, the O_2 clearly disappears and H_2 is produced, at a faster rate after all the O_2 has been consumed. The temporary placing of the system under vacuum ($P_{tot} < 10^5$ Pa) during the initial consumption of O_2 is the salient feature of this simulation. In the latter case, $P(O_2)$ increases slightly and steadily like $P(H_2)$. The pressure of N_2 (inert) remains constant in all cases.

Hence, the simulation reveals the disappearance of O_2 in the presence of Ca, reflecting the assumption of the immobilization of H_2O_2 in a calcium peroxide. It shows that an indirect and non-negligible consequence is the approximately twice as rapid pressure buildup of H_2

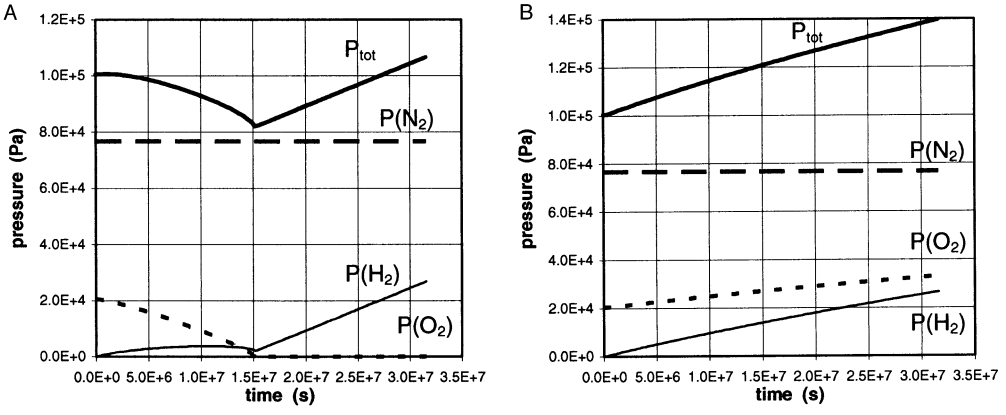

FIG. 5.
Evolution of gas pressures in a confined specimen of irradiated Portland cement paste; duration 1 year, γ dose rate 0.01 Gy s^{-1}, simulations with Ca (*A*) and without Ca (*B*).

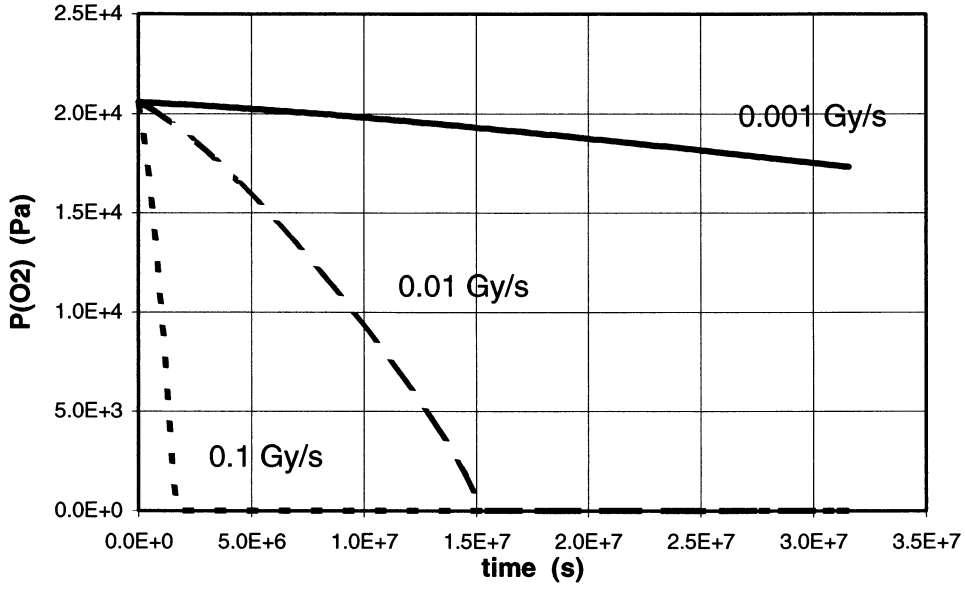

FIG. 6.
Consumption kinetics of O_2 in Portland cement paste for different γ dose rates (simulation conditions identical to Fig. 5).

when O_2 is completely consumed. The kinetic approach also helps to show that the disappearance time is shorter with the higher dose rate (Fig. 6): slightly under 6 months at 0.01 Gy s^{-1} and 18 days at 0.1 Gy s^{-1}.

Discussion

The disappearance of the dioxygen in "concrete" under irradiation finally is interpreted by the superimposition of redox reactions in solution and the precipitation of a solid phase as part of the following schematic sequence:

$$O_2 \rightleftarrows O_2^- \rightleftarrows O_2^{2-}$$

The "isolation" of the final term in an insoluble solid causes a rapid rightward shift of all the equilibria, resulting in a complete redistribution of all the oxygenated species in the interstitial liquid (pursuant to the moderation law of Le Châtelier):

$$O_2 \rightarrow O_2^- \rightarrow \textcircled{O_2^{2-}}$$

During this evolution, the pair O_2^-/O_2 always imposes its negative potential, and it is striking to observe that the concentrations calculated by CHEMSIMUL, with the help of the Nernst equation, lead to the order of magnitude found by (6):

$$E = E^{0}_{O_2^-/O_2} + 0.0592 \cdot \log_{10} \frac{[O_{2aq}]}{[O_2^-]}$$

After 1 year, calculated E is thus −0.25 and −0.67 V (SHE), with dose rates of 10^{-3} and 10^{-1} Gy s^{-1}, respectively.

The finite stock of calcium subject to peroxidation and the instability of the solid peroxide, which characterize the final step, also help to explain two types of observations reported in (6). If the dose rate is very high (2.78 Gy s^{-1}) and the dose reaches the considerable value of 2×10^7 Gy, O_2 is again produced by the cement paste. This would imply that the entire stock of Ca available is peroxidised. However, if irradiation is stopped, primary H_2O_2 is no longer produced and $CaO_2 \cdot 8H_2O$ decomposes, allowing the restoration of the redox equilibria and the progressive rise in potential (Fig. 1). The very limited lifetime of CaO_2 finally explains why this compound remains unperceived during off-line investigations, particularly after C-S-H attack (and not portlandite) by H_2O_2 in low concentration (7).

Conclusion

The radiolysis of water yields electrons and primary H_2O_2, which are O_2 reducers and precursors, respectively. When the concrete is irradiated, the consumption of oxygen results from the deep disequilibrium affecting the resulting redox sequence: dioxygen$^{(0)} \Leftrightarrow$ superoxide$^{(-1/2)} \Leftrightarrow$ peroxide$^{(-1)}$. The calcium of the medium, by capturing most of the peroxides in a very slightly soluble solid phase ($CaO_2 \cdot 8H_2O$) is responsible for this, although the sharp decrease in the oxygenated species in the interstitial liquid does not prevent the reaction $O_2 + e^-_{aq} \rightarrow O_2^- + H_2O$ from imposing a clearly reducing character on the system. The presence of calcium has major consequences for the progress of radiolysis because, in the short term, H_2 formation is slowed down and the system is placed under slight negative pressure, whereas in the long term, this formation is accelerated. This means that the long-term estimation of the quantities of radiolytic H_2 removed, as well as the estimation of the pressures reached, can neither be extrapolated from short irradiation experiments nor determined from conventional calculations, which ignore calcium. The kinetic approach to modeling remains pertinent, provided the reaction rate of Ca with H_2O_2 and the quantity of Ca actually available according to the type of material are known. The withdrawal of calcium needed for the formation of CaO_2"$8H_2O$ takes place at the expense of portlandite and ettringite, which could lead to their elimination in case of very high doses. The instability of $CaO_2 \cdot 8H_2O$ in the absence of H_2O_2, or if irradiation is stopped, makes its characterization difficult. The solubility product has nevertheless been determined and is equal to 2.8×10^{-11}.

References

1. N.E. Bibler and E.G. Orebaugh, Report DP-1459, Savannah River Laboratory (1977).
2. C.R. Wilding, D.C. Phillips, C.E. Lyon, S.G. Burnay and W.E. Spindler, Report AERE-R13756 (1990).
3. E. Bjergbakke, K. Sehested, O.L. Rasmussen and N. Christensen, Report RISØ M-2430, Risø National Laboratory (1984).
4. P. Offermann, Mater. Res. Soc. Symp. Proc. 127, 461 (1989).

5. A.B. Ross, W.G. Mallard, W.P. Helman, G.V. Buxton, R.E. Huie and P. Neta, Solution kinetics data base, Version 2.0. NIST. Gaithersburg, USA (1994).
6. M. Atkins, Nuclear Science and Technology, Final Report EUR 13542 EN, 103, Commission of the European Communities (1991).
7. K. Brodersen and K. Nilsson, Nuclear Science and Technology, Progress Report EUR 12077 EN/1, Commission of the European Communities (1987).
8. B.H.J. Bielski, D.E. Cabelli and R.L. Arudi, J. Phys. Chem. Ref. Data 14, 1041 (1985).
9. P.A. Giguére in «compléments au nouveau traité de chimie minérale» Ed. Masson (1975).
10. G.V. Buxton, C.L. Greenstock, W.P. Helman and A.B. Ross, J. Phys. Chem. Ref. Data 17, (1988).
11. P. Bouniol and P. Thouvenot, J. Chim. Phys. 94, 410 (1997).
12. P. Pascal. Nouveau traité de chimie minérale, vol. IV, Masson édit. (1958).
13. H. Remy, Lehrbuch der anorganischen Chemie, Leipzig (1960).
14. O.L. Rasmussen, E. Bjergbakke, B. Lynggaard, P. Pagsberg and P. Kirkegaard, CHEMSIMUL Version 9306, Risø National Laboratory, Denmark (1993).
15. J. Jacq and O. Bloch, Electrochim. Acta 15, 1945 (1970).
16. A.J. Elliot, and M.P. Chenier, J. Nucl. Mater. 187, 230 (1992).
17. M.H. Hutchinson and T.K. Sherwood, Ind. Eng. Chem. 29, 836 (1937).